Contribution of glacial melt to river runoff as determined by stable isotopes at the source region of the Yangtze River, China

Zhaofei Liu, Zhijun Yao and Rui Wang

ABSTRACT

The primary objective of this study was to quantify the contribution of glacial melt to total runoff in the Gaerqu River catchment, which is located in the source region of the Yangtze River, China. The isotope hydrograph separation method was used to separate glacier melt runoff from total runoff in the catchment. The degree-day method was used to investigate temporal variations in glacial melt runoff. The results showed that the contribution of glacial melt runoff to total runoff was 15.0%. The uncertainty of the separation was ± 3.7% at the confidence level of 95%. Glacial melt runoff was mainly generated in June, July, and August. The runoff coefficient was 0.23 for the catchment. Precipitation-induced runoff constituted 19.9% of the total precipitation, meaning that precipitation loss was >80% across the study period (a hydrological year). The Local Meteoric Water Line (LMWL) of the catchment was fitted as $\delta^2H = 7.75\ \delta^{18}O + 5.93$. This line has a smaller slope and intercept than the Global Meteoric Water Line. The regression-lines for the $\delta^{18}O$ and δ^2H values of stream water indicated that evaporation was greater over the entire catchment than it was for the upstream region alone.

Key words | degree-day, glacial melt, isotope hydrograph separation, LMWL, Qinghai–Tibet Plateau, stable isotope

Zhaofei Liu
Zhijun Yao (corresponding author)
Rui Wang
Institute of Geographic Sciences and Natural Resources Research,
Chinese Academy of Sciences,
100101,
Beijing,
China
E-mail: *yaozj@igsnrr.ac.cn*

INTRODUCTION

Hydrograph separation is a technique that is used for identifying runoff components, and the derived data are essential for the optimal protection of water resources, for eco-hydrological studies, and for improving flood forecasts (Wels *et al.* 1991; Wenninger *et al.* 2004). Both chemical and isotopic tracers have been widely applied in hydrograph separation. Isotopic tracers are assumed to be conservative, while chemical tracers are considered to be quasi-conservative (Richey *et al.* 1998). Various studies have compared the use of chemical and isotopic tracers and have observed differing results. Some studies found no systematic bias in isotopic or chemical hydrograph separation results (Wels *et al.* 1991; Leaney *et al.* 1993; Pionke *et al.* 1993; Ribolzi *et al.* 1996), while others observed significant differences between chemical tracer-based and isotope-based hydrograph separation results (Hooper & Shoemaker 1986; Nolan & Hill 1990; Durand *et al.* 1993; Klaus & McDonnell 2013). These differences are usually attributed to the non-conservative behavior of chemical tracers (Hooper & Shoemaker 1986). In other words, the differences are due to the fact that the reaction rates of chemical tracers can differ in different environments (Wels *et al.* 1991). Such results show the clear limitations of chemical tracers and have motivated many researchers to use isotopic tracers in hydrograph separation studies (e.g., Klaus & McDonnell 2013).

Different water types in the hydrological cycle have distinct isotopic fingerprints, and therefore, environmental isotopes can be used to identify water sources, study water

doi: 10.2166/nh.2015.089

mass movement, and understand many other hydrological processes (Kendall & Caldwell 1998; Yurtsever 2000). Stable isotopic tracers such as oxygen-18 (^{18}O) and deuterium (^{2}H) are ideal conservative tracers because they are part of the water molecule and are only subject to changes due to mixing (Klaus & McDonnell 2013). Isotopic tracers have been the most useful tool employed to identify water sources and related information, especially for the identification of runoff components (McGuire & McDonnell 2008; Gimeno *et al.* 2012).

In general, stable isotope hydrograph separation is a technique based on the assumptions that stream water is a mix of individual water sources and that the specific water sources contributing to river runoff at a particular location are known (Dincer *et al.* 1970; Maurya *et al.* 2011). Stable isotopes are generally used for two-component hydrograph separation on an event timescale, while for three-component hydrograph separation, isotopic tracers must be combined with chemical tracers (Ladouche *et al.* 2001).

Isotopic tracers have been commonly applied to identify event (new) water and pre-event (old) water (e.g., Fritz *et al.* 1976; Sklash *et al.* 1976; Sklash & Farvolden 1979; Lakey & Krothe 1996; Ladouche *et al.* 2001; Huth *et al.* 2004; Lyon *et al.* 2009; Zhao *et al.* 2013; Dahlke *et al.* 2014) by using the two-component mixing model, which is based on mass balance equations (Pinder & Jones 1969). Some studies have also used this method to separate overland (surface) flow and base (subsurface) flow (Hooper & Shoemaker 1986; Kennedy *et al.*, 1986; Hinton *et al.*, 1994; Soulsby 1995), which are considered similar to event and pre-event water, respectively. For investigating the contribution of snow/glacial melt runoff to the total runoff, the two-component and three-component hydrograph separation methods have both been applied to glacierized regions (Dincer *et al.* 1970; Shanley *et al.* 2002; Williams *et al.* 2006; Maurya *et al.* 2011; Kong & Pang 2012). Most of these studies were based on individual rainfall or snow/glacial melt events. The isotopic compositions of these individual events exhibit marked temporal variations (Qu *et al.* 2014). Although there are spatial and temporal variations in the isotopic character of water components including precipitation and streamflow, these variations are reduced when seasonal averages of isotope values over the catchment are used (Maurya *et al.* 2011). Furthermore, the annual mean contribution of different water sources is more important from the perspective of water resource management and protection than that for an individual event. Therefore, seasonal mean isotopic data is recommended for use in hydrograph separation.

The source region of the Yangtze River (SRYR), which is located in the interior of the Qinghai–Tibet Plateau, is a unique natural environment with abundant natural resources that also serve important ecological functions. The natural surrounding environment and the aquatic ecosystem are both very fragile and linked to water availability. Glacial retreat, albeit with strong regional variability, has been observed on the Qinghai–Tibet Plateau (Yao *et al.* 2004). While magnitudes have varied, glaciated areas at the SRYR have shrunk during the past four decades (Ye *et al.* 2006; Zhang *et al.* 2008; Wu *et al.* 2013; Yao *et al.* 2014). Changes to the region's glaciers can ultimately affect the ecosystem as well as have an impact on regional water resources at the SRYR. Therefore, it is essential to investigate the contribution of glaciers to total runoff.

In this study, a seasonal stable isotope dataset (from the observational period 1 June 2013 to 10 June 2014), for precipitation, glacial meltwater, and streamflow was applied to the isotope hydrograph separation method to quantify the contribution of glacial meltwater to total runoff in a high altitude catchment of the Gaerqu River, which is located in the SRYR, China. This study focused on quantifying the contributions of the two different water sources (precipitation and glacial meltwater) identified in the streamflow at the catchment outlet. Soil water, also known as base flow or groundwater, is also a product of precipitation and glacial meltwater. Therefore, soil water movement via hydrological processes was not reflected in the results.

Because of the harsh natural environment, the study area has not been affected much by human activities such as land use change. This was beneficial for our scientific research. In this study, the hydro-meteorological variables observed included precipitation, air temperature, and streamflow. Water samples of precipitation, glacial melt, and river water were collected and analyzed for stable isotopes. With the results of these analyses, the isotope hydrograph separation method was used to quantify the contribution of glacial melt to total runoff during the entire observational period. Finally, the degree-day method was

applied to investigate temporal variations in glacial melt runoff. It is hoped that the results of this study will provide a useful resource to support water resource management and protection efforts, especially as the SRYR undergoes glacial changes.

MATERIALS AND METHODS

Study area

The SRYR is located in the central eastern part of the Qinghai–Tibet Plateau. With an average altitude of 4,754.5 m above sea level (a.s.l.), this region includes one of the highest major river basins in the world. Glaciers of the SRYR are primarily distributed on the northern slope of the Tanggula Mountains, the southern slope of the Kunlun Mountains, and on Sedir Mountain. According to the Chinese Glacier Inventory (Shi *et al.* 2005), 753 glaciers are located in the SRYR, and these have a combined total volume in water equivalents of approximately 887.5×10^8 m^3, which is five times the annual discharge of the SRYR.

The Gaerqu River is one of main headwater rivers of the SRYR. Its catchment area is 4,482.0 km^2 and has a mean altitude of ~5,015.4 m a.s.l. (with a total altitude range of 4,491 to 6,621 m a.s.l). The arid to semi-arid climate of the catchment results from its location and from the topographical features of the Qinghai–Tibet Plateau. Mean annual precipitation is <300 mm, and precipitation falls mainly between June and September coincident with the annual peak of glacial melt for the region. Because of the high altitude, the environment of the catchment is very cold. The mean air temperature between June 2013 and June 2014 was −3.7 °C. The mean values of the daily maximum and minimum air temperatures during the same period were 5.1 °C and −10.0 °C, respectively. Rivers are frozen during the winter season (DJF).

Observational data and sample collection

Between June 2013 and June 2014, the catchment was equipped with automatic observation instruments to observe precipitation, air temperatures, river water levels, and water temperatures (Figure 1). The time interval used for recording precipitation and air temperatures was 6 hours, while the time interval used for river water levels and water temperatures was 3 hours. Two Onset water level loggers were installed at two discharge locations in order to measure the downstream flow and the upstream flow, respectively (shown as 'Discharge 1' and 'Discharge 2' in Figure 1). However, only the logger at Discharge 2 provided data for this study; the logger at Discharge 1 was lost presumably because of natural reasons. River discharge (or streamflow) at the catchment outlet was measured using a FlowQuest 2000 acoustic current profiler during June 2013, August 2013, and May 2014, which represented time periods of normal flow, ample flow, and low flow, respectively. FlowQuest 2000 is highly accurate at measuring river channel discharge from shallow to medium water depths. In general, results show a rope relation between discharge and water level for a river cross-section. The rope relation curve includes a rising flow and a recession flow, with one water level corresponding to the rising flow and another corresponding to the recession flow.

Water samples, including those for precipitation, glacial melt, and river water, were collected during the observational period. Precipitation samples were collected for each precipitation event (including rainfall and snowfall) at the observation sites (Figure 1). Samples of glacial meltwater were collected at the Geladandong Glacier, which supplies runoff to the catchment. The numbers of water samples for precipitation, glacial melt, and river water were 12, 42, and 40, respectively.

Landsat 8 Operational Land Imager (OLI) and Landsat Enhanced Thematic Mapper Plus (ETM+) imagery data were analyzed to detect glacier margins in the catchment. The Landsat imagery data were obtained from http://glovis.usgs.gov/. The images (Path 138 and Row 037) covered the entire catchment. In total, four images were obtained, including two OLI images (May 21, 2013 and September 10, 2013) and two ETM+ images (August 1, 2013 and July 3, 2014).

Measurement of stable isotopes

The stable isotopes of precipitation and river water samples were analyzed using a liquid-water isotope analyzer (Picarro L2120-i) at the Institute of Geographic Sciences and Natural Resources Research, Chinese Academy of Sciences (CAS).

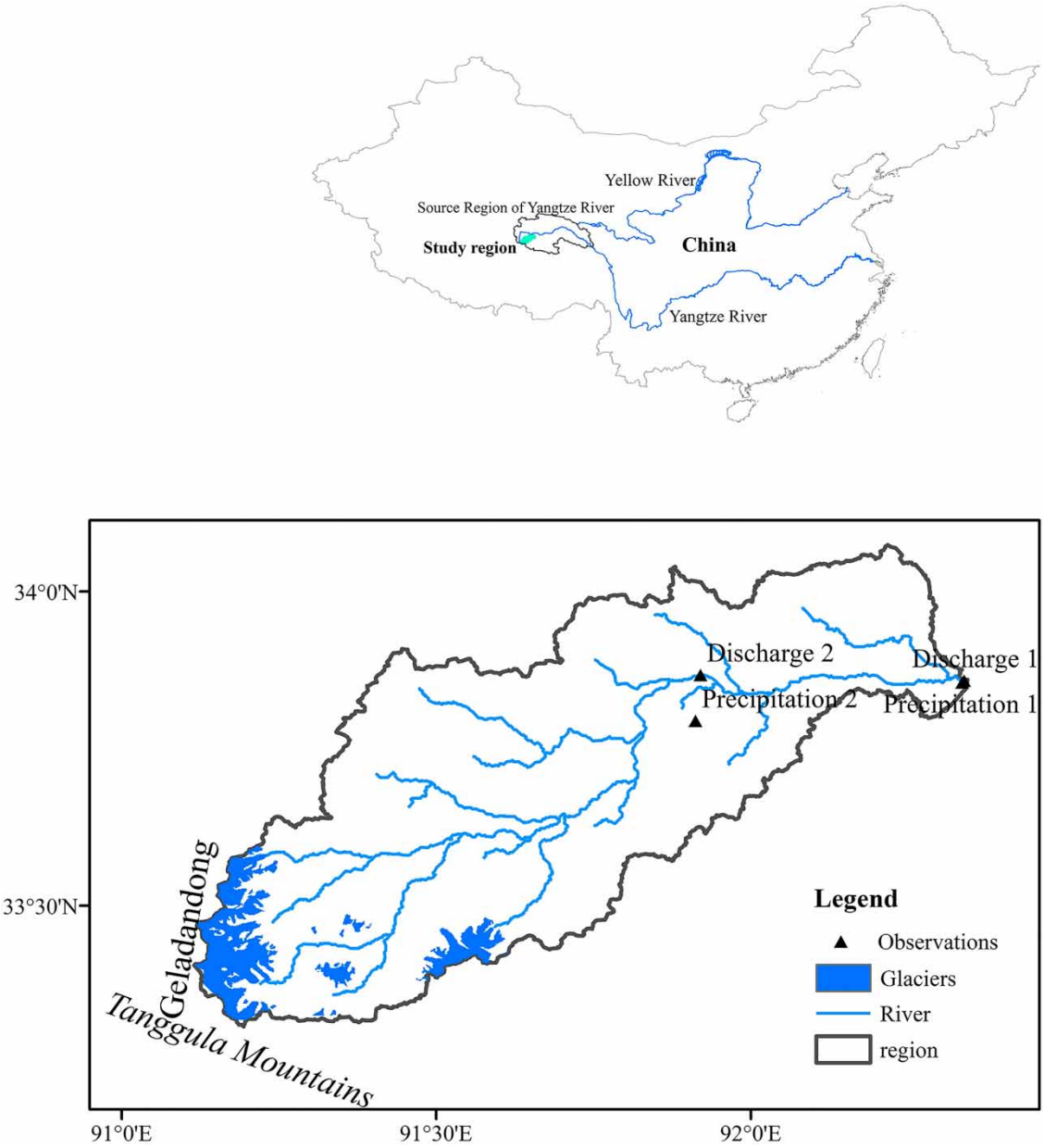

Figure 1 | Location of the study region (Gaerqu River catchment) and the sites where field observations and water samples were collected.

Isotopic ratios are expressed in the δ notation of units of per mil (‰) relative to the Vienna-Standard Mean Ocean Water (V-SMOW; Gonfiantini 1978):

$$\delta = \left(\frac{R_{\text{sample}}}{R_{\text{SMOW}}} - 1\right) \times 10^3 \quad (1)$$

where R is the ratio $^{18}O/^{16}O$ or $^{2}H/^{1}H$.

The Picarro L2120-i provides measurements of $\delta^{18}O$ and $\delta^{2}H$ in liquid-water samples with an accuracy better than 0.2‰ for $^{18}O/^{16}O$ and 0.6‰ for $^{2}H/^{1}H$. Both $\delta^{18}O$ and $\delta^{2}H$ were measured for all water samples with the exception of glacial melt. Glacial meltwater samples were analyzed for $\delta^{18}O$ alone using the Picarro L2120-i at the Institute of Tibetan Plateau Research, CAS.

Isotope hydrograph separation

The physically based hydrograph separation method was selected to separate the water sources of runoff into precipitation and glacial melt, but this was done without consideration for underground water movement via hydrological processes (e.g., groundwater). This method is based on calculating the mass balance of isotopic tracer fluxes and water. The balance equations used for the hydrograph separation method are as follows:

$$Q_t = Q_p + Q_g \tag{2}$$

$$\delta_t Q_t = \delta_p Q_p + \delta_g Q_g \tag{3}$$

where Q_t is the total runoff (represented by the streamflow at the catchment outlet in m^3s^{-1}), Q_p and Q_g are the contributions to streamflow from precipitation and glacial meltwater (m^3s^{-1}), respectively, δ_t is the isotopic concentration of total runoff (‰), and δ_p and δ_g are the isotopic concentrations for the precipitation and glacial meltwater runoff components (‰), respectively. Based on Equations (2) and (3), a two-component separation model was used to identify contribution of glacial melt runoff as follows:

$$f_g = \frac{Q_g}{Q_t} = \frac{\delta_p - \delta_t}{\delta_p - \delta_g} \tag{4}$$

As a result of limited data availability, only $\delta^{18}O$ values were used for the isotope hydrograph separation in this study. Past studies have suggested that ^{18}O provides more reliable results than ^{2}H (Rozanski *et al.* 2001).

The uncertainty of the isotope hydrograph separation for two components was calculated using the method proposed by Genereux (1998). Assuming that a parameter y is a function of several variables $x_1, x_2, \ldots, x_n$ (i.e. $y = f(x_1, x_2, \ldots, x_n)$), and the uncertainty in each variable is independent of the uncertainty in the others, the uncertainty in y is related to the uncertainty in each of the variables by the following:

$$Wy = \sqrt{\left(\frac{\partial y}{\partial x_1} W_{x1}\right)^2 + \left(\frac{\partial y}{\partial x_2} W_{x2}\right)^2 + \cdots + \left(\frac{\partial y}{\partial x_n} W_{xn}\right)^2} \tag{5}$$

where W represents the uncertainty in the variable specified in the subscript. Application of Equations (5) and (4) showed the uncertainty as

$$W_{f_g} = \sqrt{\left(\frac{\delta_p - \delta_t}{\delta_p - \delta_g} W_{C_m}\right)^2 + \left(\frac{\delta_t - \delta_g}{\delta_p - \delta_g} W_{C_p}\right)^2 + \left(\frac{-1}{\delta_p - \delta_g} W_{C_t}\right)^2} \tag{6}$$

where the uncertainty W is estimated for using standard deviations multiplied by t values from the Student's distribution.

Delineation of glacier areas

Glacier margins were identified using remote sensing images. Manual interpretation, which has proved to be the best method for delineating glacier areas from satellite imagery (Bishop *et al.* 2004; Raup *et al.* 2007), was selected to delineate glacier boundaries in the catchment. This method is particularly effective when delineation is conducted by the same person using a combination of different types of imagery (Paul *et al.* 2002). Glacial areas were manually digitized from satellite images using the software ArcGIS 10.0. Glacier outlines were mapped manually by using false color composite bands.

Degree-day method

The degree-day method was applied to investigate temporal variations in glacial melt runoff. This method is based on the concept that glacier melting occurs when the mean air temperatures above the glacier surface are above the melting point of ice (0 °C). Therefore, the total melt runoff during a particular period is proportional to the sum of the positive mean air temperatures for the same period (Braithwaite & Raper 2007; Hughes & Braithwaite 2008). The degree-day method is calculated as follows:

$$M = \mathrm{DDF} \times T^+ \tag{7}$$

$$\sum_{i=1}^{n} M_i = \mathrm{DDF} \times \sum_{i=1}^{n} T_i^+ \tag{8}$$

where M is glacial meltwater (m^3/d), T^+ is the positive air temperature (°C), n is the number of daily samples of the

glacial meltwater, and DDF is the degree-day factor ($m^3\,^\circ C^{-1}d^{-1}$). These calculations were performed on daily data series. The DDF was calibrated by Equation (8).

In this study, the unit used for the DDF was $m^3\,^\circ C^{-1}d^{-1}$ and not $mm^\circ C^{-1}d^{-1}$, which has been used often in other studies. This choice was made because the chosen unit is more convenient for calculating glacial melt runoff. Due to data limitations, the revised degree-day method, which requires more datasets (including radiation data), was not used in this study.

Based on the observed air temperature data, the air temperature lapse rate at the Dongkemadi Glacier was identified as 0.63 °C/100 m and 0.67 °C/100 m by Liu *et al.* (2006) and Qiao *et al.* (2010), respectively. The Dongkemadi Glacier is located in the Tanggula Mountains of the SRYR, and it is near to the Geladandong Glacier (the glacier used in this study). A mean air temperature lapse rate of 0.65 °C/100 m was used as the air temperature lapse rate for the study area. This value was subsequently used to calculate the air temperature at the glacier margin, as identified from remote sensing imagery.

RESULTS

Hydrological characteristics of the Gaerqu River catchment

The observed water levels and corresponding streamflow for the Gaerqu River catchment are shown in Figure 2. In this study, the rising flow and recession flow were fitted by a logarithmic curve and an exponential curve, respectively. The streamflow at the catchment outlet corresponding to each water level was then calculated from this rope relation curve.

Streamflow at observation site Discharge 1 ranged between 9.5 and 22.9 m^3/s, with a mean value of 15.8 m^3/s. The river was frozen from November 7, 2013 to April 28, 2014. The mean air temperature and water temperature during this period were −7.7 °C and −5.4 °C, respectively. The hydrograph of the catchment outlet during the observation period is shown in Figure 3. In spring 2014, the river melted at the end of April, as shown in the hydrograph of the catchment outlet for the observation period (Figure 3).

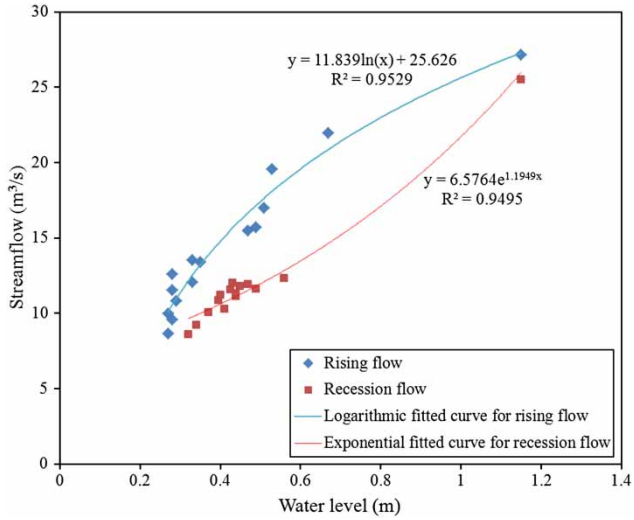

Figure 2 | Rope relation curve between discharge and water level at the catchment outlet.

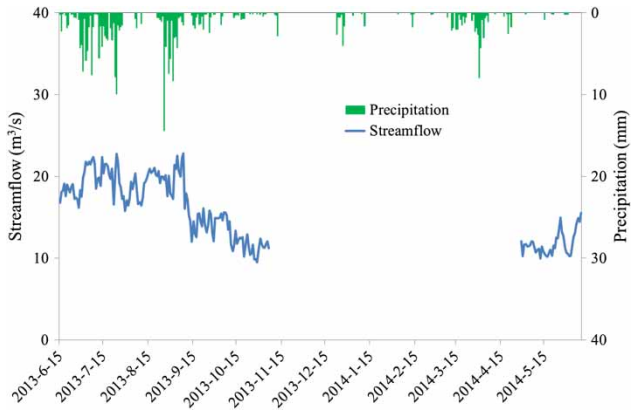

Figure 3 | Hydrograph of the Gaerqu River catchment at the observation station named 'Discharge 1' during June 15, 2013–June 10, 2014.

A sharp increase in flow occurred in early June 2014. Together with the streamflow data in June 2013, these data span a hydrological year for the whole observation period.

The observed streamflow was greatest from July to early September coincident with the highest precipitation and highest air temperatures recorded during the hydrological year. The maximum flow during the observation period was 22.9 m^3/s, and this occurred on September 8, 2013. Streamflow dropped abruptly in mid-September from a mean of 19.7 m^3/s (plentiful flow period: July–early September) to a mean of 12.9 m^3/s (normal flow: mid September–November). The river froze in November. This abrupt change was facilitated by the rapid decrease in precipitation

levels in the catchment. Despite little difference in precipitation between this normal water flow period and June 2013, the streamflow in June 2013 was clearly larger. This increase was likely driven by the seasonal snowmelt that occurs in May–June, when the mean air temperatures are above 0 °C. This would also explain the peak river flow observed in May 2014, despite little precipitation.

In summary, the hydrograph showed a strong correlation between streamflow and precipitation, with the correlation coefficient (R) being 0.86. However, glacial melt runoff could also explain some of the observed streamflow variations, since there was also a positive relationship between streamflow and the mean air temperature ($R = 0.73$), and air temperature was positively correlated with glacial melt runoff ($R = 0.998$).

During the hydrological year, total runoff was $\sim 2.6 \times 10^8$ m^3, which is equivalent to 57.0 mm of precipitation. The total precipitation observed during the hydrological year was 243.9 mm, which is equivalent to $\sim 10.9 \times 10^8$ m^3. Based on precipitation alone, the runoff coefficient, as defined by the ratio of annual runoff to precipitation, was 0.23 for the catchment. If glacial melt runoff was not included, the hydrological budget equation could be described as that precipitation subtracted by runoff was equal to the sum of evapotranspiration and changes in soil water storage at a catchment. This value suggests that precipitation accounted for <25% of runoff throughout the hydrological year, with the remainder lost to evapotranspiration or to changes in soil water storage in the catchment. However, in reality, the precipitation loss must be >76.6% because the true runoff coefficient reflects the combination of both precipitation and glacier melt.

Isotopic compositions of water samples and environmental implications

The correlations between δ^{18}O and δ^2H values of precipitation and stream water during the observation period are shown in Figure 4. The Local Meteoric Water Line (LMWL) of the Gaerqu River catchment was obtained from the isotope values of precipitation samples at the two precipitation observation sites (Figure 1).

The line was fitted as $\delta^2\text{H} = 7.75\ \delta^{18}\text{O} + 5.93$, with a regression line R^2 value of 0.98. The slope was close to

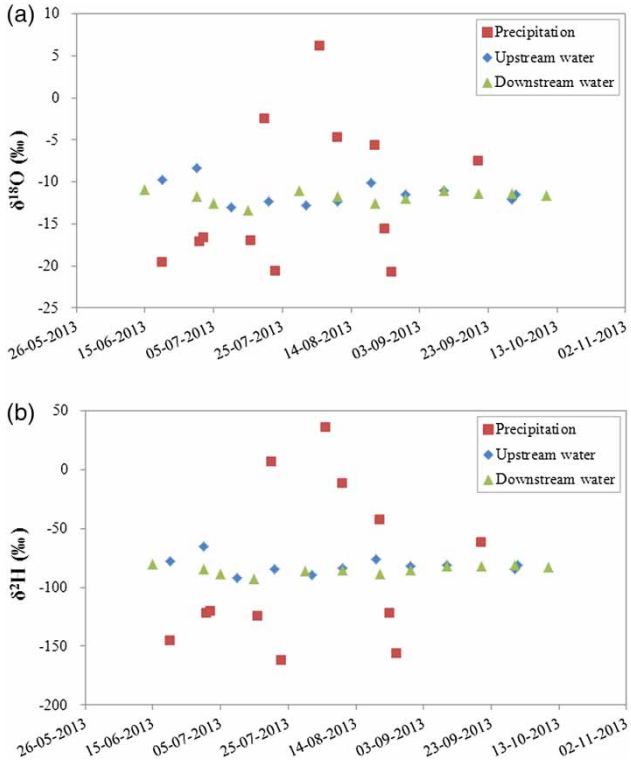

Figure 4 | Correlation between the δ^{18}O and δ^2H values of precipitation and stream water during the observation period.

that of the Tingri station (Kang *et al.* 2002), which was in the northern slope of the Himalayas. The LMWL of the study area had a smaller slope and intercept as compared to the Global Meteoric Water Line (GMWL, $\delta^2\text{H} = 8\ \delta^{18}\text{O} + 10$), as defined by Craig (1961). The catchment is located on the north slope of the Tanggula Mountains, which is a barrier for Indian Ocean moisture transport. Before water vapor transport to the catchment, isotopic fractionation during processes of precipitation and evaporation made losses of heavy isotope (^{18}O and δ^2H). This included the continental effect, the latitude effect, and the altitude effect. These processes likely led to the smaller intercept of the LMWL as compared with the GMWL. The depletion rate of δ^2H during isotopic fractionation is larger than that of δ^{18}O. This resulted in the smaller slope of the LMWL as compared with the GMWL.

During the observation period, the δ^{18}O and δ^2H values of precipitation ranged from −20.8‰ to 6.1‰ and from −161.9‰ to 36.1‰, respectively. A scatter plot for precipitation amount and δ^{18}O values of precipitation is

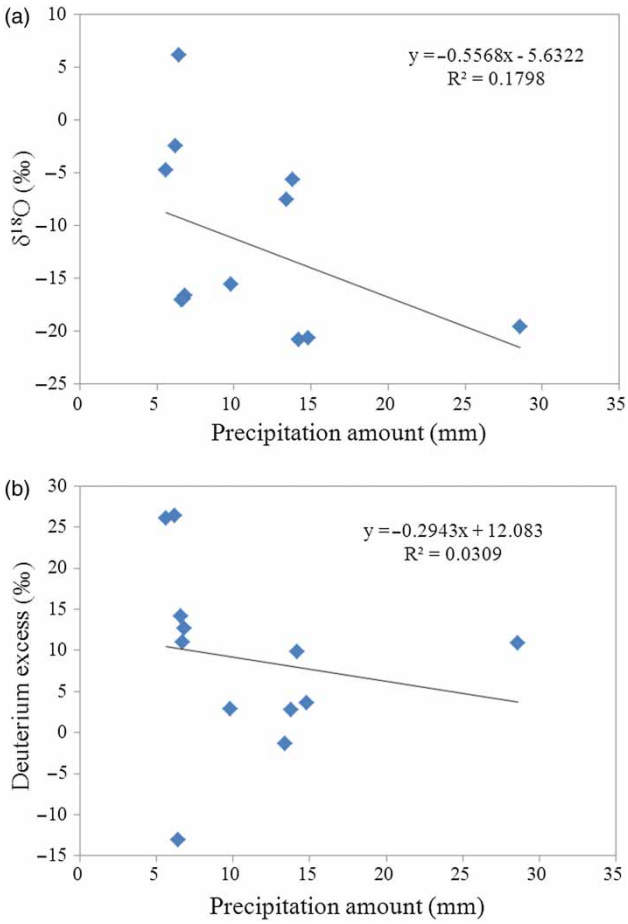

Figure 5 | Correlation between precipitation amount and (a) $\delta^{18}O$ values of precipitation and (b) deuterium excess.

shown in Figure 5. In general, it shows a negative correlation between precipitation amount and $\delta^{18}O$ values of precipitation at the studied region. This was consistent with other studies over the Qinghai–Tibet Plateau (Tian *et al.* 1996; Kang *et al.*, 2000, 2002). However, it could be seen from the figure that there were no significant relationships between $\delta^{18}O$ and daily precipitation amount. It was also consistent with that at Tingri station (Kang *et al.* 2002). In contrast to precipitation samples, the ranges for the $\delta^{18}O$ and $\delta^{2}H$ isotopic compositions of stream water were much lower at both sampling sites. The fitted lines for upstream water and downstream water were expressed as $\delta^{2}H = 4.89\ \delta^{18}O–26.34$ and $\delta^{2}H = 5.21\ \delta^{18}O–22.96$, with regression line R^2 values of 0.93 and 0.94, respectively. Over the course of the hydrological cycle, the volume of stream water is proportional to the volume of water in the catchment after evaporation. Therefore, the regression line of stream water represents the degree of evaporation in the catchment. The results indicate that the proportion of water lost to evaporation across the study catchment was greater than that observed for the upstream region alone.

Isotope hydrograph separation and its uncertainty

During the observation period, the volume-weighted mean values of $\delta^{18}O$ for streamflow at the catchment outlet, for the precipitation at the two sample sites, and for glacial meltwater were −11.9‰, −11.3‰, and −15.6‰, respectively. Calculations using the isotope hydrograph separation method, Equation (4), show that the contribution of glacial melt runoff to total runoff was 15.0%. Uncertainty results for hydrograph separation were shown in Table 1. Calculated by Equation (7), the uncertainty of the separation was ± 3.7% at the confidence level of 95%. Therefore, the contribution of glacial melt runoff was 15.0 ± 3.7% (the confidence level of 95%) at the Gaerqu River catchment. As the total runoff during the observation period was 2.55×10^8 m^3, the glacial melt runoff can be calculated as $(0.38 \pm 0.09) \times 10^8$ m^3.

The sum of positive air temperatures at the glacier margin during the observation period was 312.7 °C. Based on Equation (8), the DDF was calculated as 1.2×10^5

Table 1 | Statistics of the $\delta^{18}O$ values and uncertainty results for hydrograph separation

Samples	Number of samples	Weighted mean $\delta^{18}O$ (‰)	Standard deviation	t (95%)	Uncertainty (95%)
Precipitation	12	−11.3	8.3	2.201	18.246
Glacier	42	−15.6	4.8	2.020	1.436
Streamflow	24	−11.9	0.7	2.069	9.740

Note: 95% represents the confidence level.

$m^3d^{-1}\,^{\circ}C^{-1}$. This DDF value was used to calculate a daily time series of glacial melt runoff according to the positive air temperatures. The results show temporal variations in the contribution of glacial meltwater to total flow at the catchment outlet (Figure 6). Glacial melt runoff is mainly generated in June, July, and August. In 2014, glacial melt runoff started at the beginning of June coincident with the onset of positive air temperatures. In 2013, glacial melt runoff ended at the beginning of September. The results show that the largest glacier melt runoff occurred in August 2013, with a total of 15.4×10^6 m^3 recorded across the month. The greatest daily glacial melt runoff value calculated was 1.0×10^6 m^3 on August 18, 2013.

DISCUSSION

The runoff coefficient for the catchment was calculated as 0.23, which indicates that runoff constituted 23% of the total precipitation throughout the study period (a single hydrological year). Since the contribution of glacial melt runoff to total runoff was calculated as 15.0%, the contribution of precipitation to total runoff was 85.0%. Then, runoff coming from precipitation was calculated as the total runoff multiplied by 85.0%. Therefore, precipitation-induced runoff constituted 19.9% of the total annual precipitation, meaning that precipitation loss was <80% across the hydrological year. Precipitation was mainly lost due to evapotranspiration or changes in soil water storage in the catchment.

The LMWL of the Gaerqu River catchment was fitted as $\delta^2H = 7.75\ \delta^{18}O + 5.93$. This line had a smaller slope and intercept as compared to the GMWL. During the transportation of marine moisture to the catchment, stable isotopes ($\delta^{18}O$ and δ^2H) were depleted due to the continental effect, the latitude effect, and the altitude effect. These processes led to the smaller intercept of the LMWL as compared with the GMWL. The depletion rate of δ^2H during isotopic fractionation was larger than that of $\delta^{18}O$, which resulted in the smaller slope of the LMWL as compared with the GMWL. The isotopic composition of stream water is located across the Evaporation Line. The intersection point between the Evaporation Line and the LMWL represented the remaining water on the ground after evaporation. Because of isotopic fractionation in evaporation, the remaining water was enriched with heavy isotopes (^{18}O and δ^2H). In other words, the enrichment of ^{18}O and δ^2H had a positive correlation with evaporation. For the intersection point, the $\delta^{18}O$ and δ^2H values were more enriched at downstream water than that at upstream water. This indicated evaporation was greater over the entire catchment than that for the upstream region alone. It is possible that this reflects the lower mean air temperatures of the upstream region.

When applying the isotope hydrograph separation method, the use of mean isotopic values calculated over a

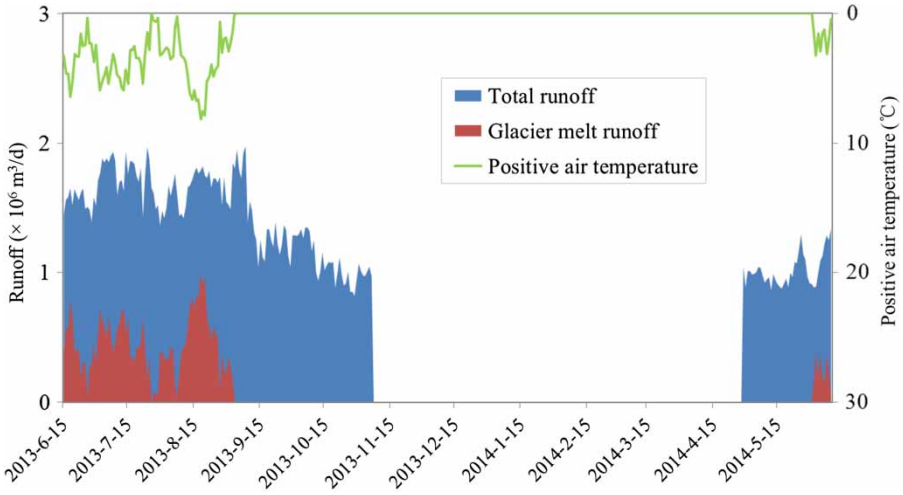

Figure 6 | Temporal variations in the contribution of glacial melt runoff to total runoff in the Gaerqu River catchment.

long period can help to reduce the uncertainties caused by the lag time of flow concentrations. Applying the isotope hydrograph separation method to precipitation-runoff events is difficult because they are affected by a lag time of flow concentration. However, in this study, river water samples were not collected immediately after every precipitation event, and as a result, isotope hydrograph separations for individual precipitation-runoff events were not included in this study.

Hydrograph separation was focused on the contribution of the initial sources of runoff in the catchment (precipitation and glacial melt) to the total runoff. The isotopes in river water reflect the initial water sources. In this study, isotopic movement through other hydrological processes was not considered, for example, isotope fractionation during the evaporation process.

In this study, it was assumed that glacial melt originates at glacier margins and that the degree-day factor was constant at the glacier margin zone. Although glacier margins were necessarily changing as a result of glacial melt, at the altitude of this study these changes were <15 m during the observation period. Therefore, the degree-day factor at the glacier margin zone, which was identified midway through the observation period, was representative of the glacial melt characteristics across the whole period.

CONCLUSIONS

Observed hydro-meteorological data and isotope data of 94 water samples were applied using the isotope hydrograph separation method to quantify the contribution of glacial meltwater to total runoff in the Gaerqu River catchment. The degree-day method was used to detect temporal variations in glacial melt runoff. The contribution of glacial melt runoff to total runoff, as identified by the isotope hydrograph separation method, was 15.0%. Glacial melt runoff was mainly generated in June, July, and August, with the largest monthly value in August 2013 (15.4×10^6 m^3). The greatest daily glacial melt runoff recorded was 1.0×10^6 m^3, which occurred on August 18, 2013. It is hoped that the results of this study will provide a useful resource to support water resource management and protection efforts, especially as the SRYR undergoes glacial changes.

ACKNOWLEDGEMENTS

This study was supported and funded by the National Natural Science Foundation of China (Grant No. 41371058, No. 41201035, and No. 41190080). Isotope data for glacial meltwaters were provided by Prof. Shichang Kang. Thanks are also extended to Lei Wang and Liguang Jiang for assistance in the field.

REFERENCES

Bishop, M. P., Olsenholler, J. A., Shroder, J. F., Barry, R. G., Raup, B. H., Bush, A. B. G., Copland, L., Dwyer, J. L., Fountain, A. G., Haeberli, W., Kääb, A., Paul, F., Hall, D. K., Kargel, J. S., Molnia, B. F., Trabant, D. C. & Wessels, R. 2004 Global land Ice Measurements from Space (GLIMS), remote sensing and GIS investigations of the Earth's Cryosphere. *Geocarto Int.* **19**, 57–84.

Braithwaite, R. J. & Raper, S. C. B. 2007 Glaciological conditions in seven contrasting regions estimated with the degree-day model. *Ann. Glaciol.* **46**, 297–302.

Craig, H. 1961 Isotopic variations in meteoric waters. *Science* **133**, 1702–1708.

Dahlke, H. E., Lyon, S. W., Jansson, P., Karlin, T. & Rosqvist, G. 2014 Isotopic investigation of runoff generation in a glacierized catchment in northern Sweden. *Hydrol. Process.* **28**, 1383–1398.

Dincer, T., Payne, B. R., Florkowski, T., Martinec, J. & Tongiorgi, E. 1970 Snowmelt runoff from measurements of tritium and oxygen-18. *Water Resour. Res.* **6**, 110–124.

Durand, P., Neal, M. & Neal, C. 1993 Variations in stable oxygen isotope and solute concentrations in small submediterranean montane streams. *J. Hydrol.* **144**, 283–290.

Fritz, P., Cherry, J. A., Weyer, K. U. & Sklash, M. 1976 Storm run-off analysis using environmental isotopes and major ions. In: *Interpretation of Environmental Isotope and Hydrochemical Data in Groundwater Hydrology*. International Atomic Energy Agency, Vienna, pp. 111–130. Available from: http://www-naweb.iaea.org/napc/ih/documents/IAEA%20Monographs/STI%20429%20Interpretation%20environmental%20isotope%20and%20hydrochemical%20data%201976.PDF.

Genereux, D. P. 1998 Quantifying uncertainty in tracer-based hydrograph separation. *Water Resour. Res.* **34**, 915–919.

Gimeno, L., Stohl, A., Trigo, R. M., Dominguez, F., Yoshimura, K., Yu, L., Drumond, A., Durán-Quesada, A. M. & Nieto, R. 2012 Oceanic and terrestrial sources of continental precipitation. *Rev. Geophys.* **50**, RG4003. Doi:10.1029/2012RG000389.

Gonfiantini, R. 1978 Standards for stable isotope measurements in natural compounds. *Nature* **271**, 534–536.

Hinton, M. J., Schiff, S. L. & English, M. C. 1994 Examining the contributions of glacial till water to storm runoff using

2-component and 3-component hydrograph separations. *Water Resour. Res.* **30** (4), 983–993.

Hooper, R. P. & Shoemaker, C. A. 1986 A comparison of chemical and isotopic hydrograph separation. *Water Resour. Res.* **22**, 1444–1454.

Hughes, P. D. & Braithwaite, R. J. 2008 Application of a degree-day model to reconstruct Pleistocene glacial climates. *Quat. Res.* **69**, 110–116.

Huth, A. K., Leydecker, A., Sickman, J. O. & Bales, R. C. 2004 A two-component hydrograph separation for three high-elevation catchments in the Sierra Nevada, California. *Hydrol. Process.* **18**, 1721–1733.

Kang, S. C., Wake, C. P., Qin, D. H., Mayewski, P. A. & Yao, T. D. 2000 Monsoon and dust signals recorded in Dasuopu glacier, Tibetan Plateau. *J. Glaciol.* **46**, 222–226.

Kang, S. C., Karl, J. K., Paul, A. M., Qin, D. H. & Yao, T. D. 2002 Stable-isotopic composition of precipitation over the northern slope of the central Himalaya. *J. Glaciol.* **48**, 519–526.

Kendall, C. & Caldwell, E. A. 1998 Fundamentals of isotope geochemistry. In: *Isotope Tracers in Catchment Hydrology* (C. Kendall & J. J. McDonnell, eds). Elsevier, Amsterdam, pp. 51–86.

Kennedy, V. C., Kendall, C., Zellweger, G. W., Wyerman, T. A. & Avanzino, R. J. 1986 Determination of the components of stormflow using water chemistry and environmental isotopes, Mattole River basin, California. *J. Hydrol.* **84** (1–2), 107–140.

Klaus, J. & McDonnell, J. J. 2013 Hydrograph separation using stable isotopes. Review and evaluation. *J. Hydrol.* **505**, 47–64.

Kong, Y. L. & Pang, Z. H. 2012 Evaluating the sensitivity of glacier rivers to climate change based on hydrograph separation of discharge. *J. Hydrol.* **434–435**, 121–129.

Ladouche, B., Probst, A., Viville, D., Idir, S., Baque, D., Loubet, M., Probst, J. L. & Bariac, T. 2001 Hydrograph separation using isotopic, chemical and hydrological approaches (Strengbach catchment, France). *J. Hydrol.* **242**, 255–274.

Lakey, B. & Krothe, N. C. 1996 Stable isotopic variation of storm discharge from a perennial karst spring, Indiana. *Water Resour. Res.* **32**, 721–731.

Leaney, F. W., Smettem, K. R. J. & Chittleborough, D. J. 1993 Estimating the contribution of preferential flow to subsurface runoff from a hillslope using deuterium and chloride. *J. Hydrol.* **147**, 83–103.

Liu, J. F., Yang, J. P., Chen, R. S. & Yang, Y. 2006 The simulation of snowmelt runoff model in the Dongkemadi river basin, headwater of the Yangtze River. *Acta Geogr. Sin.* **61**, 1149–1159 (In Chinese).

Lyon, S. W., Desilets, S. L. E. & Troch, P. A. 2009 A tale of two isotopes, differences in hydrograph separation for a runoff event when using δD versus $\delta^{18}O$. *Hydrol. Process.* **23**, 2095–2101.

Maurya, A. S., Shah, M., Deshpande, R. D., Bhardwaj, R. M., Prasad, A. & Gupta, S. K. 2011 Hydrograph separation and precipitation source identification using stable water isotopes and conductivity, River Ganga at Himalayan foothills. *Hydrol. Process.* **25**, 1521–1530.

McGuire, K. & McDonnell, J. J. 2008 Stable isotope tracers in watershed hydrology. In: *Stable Isotopes in Ecology and Environmental Science*, 2nd edn (R. Michener & K. Lajtha, eds). Blackwell Publishing Ltd, Oxford, United Kingdom, pp. 342–343.

Nolan, K. M. & Hill, B. R. 1990 Storm-runoff generation in the Permanente Creek drainage basin, west central California, an example of flood-wave effects on runoff composition. *J. Hydrol.* **113**, 343–367.

Paul, F., Kääb, A., Maisch, M., Kellenberger, T. & Haeberli, W. 2002 The new remote-sensing-derived Swiss glacier inventory, I. Methods. *Ann. Glaciol.* **34**, 355–361.

Pinder, G. F. & Jones, J. F. 1969 Determination of the groundwater component of peak discharge from the chemistry of total runoff. *Water Resour. Res.* **5**, 438–445.

Pionke, H. B., Gburek, W. J. & Folmar, G. J. 1993 Quantifying stormflow components in a Pennsylvania watershed when 18O input and storm conditions vary. *J. Hydrol.* **148**, 169–187.

Qiao, C. J., He, X. B. & Ye, B. S. 2010 Study of the degree-day factors for snow and ice on the Dongkemadi glacier, Tanggula range. *J. Glaciol. Geocryol.* **32**, 257–264 (In Chinese).

Qu, S. M., Zhou, M. M., Shi, P., Liu, H., Bao, W. M. & Chen, X. 2014 Differences in oxygen-18 and deuterium content of throughfall and rainfall during different flood events in a small headwater watershed. *Isot. Environ. Health Stud.* **50**, 52–61.

Raup, B., Kääb, A., Kargel, J. S., Bishop, M. P., Hamilton, G., Lee, E., Paul, F., Rau, F., Soltesz, D., Khalsa, S. J. S., Beedle, M. & Helm, C. 2007 Remote sensing and GIS technology in the global land ice measurements from space (GLIMS) project. *Comput. Geosci.* **33**, 104–125.

Ribolzi, O., Vallès, V. & Bariac, T. 1996 Comparison of hydrograph deconvolutions using residual alkalinity, chloride, and oxygen 18 as hydrochemical tracers. *Water Resour. Res.* **32**, 1051–1059.

Richey, D. G., McDonnell, J. J., Erbe, M. W. & Hurd, T. M. 1998 Hydrograph separations based on chemical and isotopic concentrations, a critical appraisal of published studies from New Zealand, North America and Europe. *J. Hydrol. (NZ)* **37**, 95–111.

Rozanski, K., Froehlich, K. & Mook, W. G. 2001 Environmental isotopes in the hydrological cycle, principles and applications. Vol. 3, Surface water. http,//www-naweb.iaea.org/napc/ih/documents/global_cycle/Environmental%20Isotopes%20in%20the%20Hydrological%20Cycle%20Vol%203.pdf.

Shanley, J. B., Kendall, C., Smith, T. E., Wolock, D. M. & McDonnell, J. J. 2002 Controls on old and new water contributions to stream flow at some nested catchments in Vermont, USA. *Hydrol. Process.* **16**, 589–609.

Shi, Y., Liu, C., Wang, Z., Liu, S. & Ye, B. 2005 *Concise glacier inventory of China*. Shanghai Popular Science Press, Shanghai.

Sklash, M. G. & Farvolden, R. N. 1979 The role of groundwater in storm runoff. *J. Hydrol.* **43**, 45–65.

Sklash, M. G., Farvolden, R. N. & Fritz, P. 1976 A conceptual model of watershed response to rainfall developed through the use of oxygen-18 as a natural tracer. *Can. J. Earth Sci.* **13**, 271–283.

Soulsby, C. 1995 Contrasts in storm event hydrochemistry in an acidic afforested catchment in upland Wales. *J. Hydrol.* **170** (1–4), 159–179.

Tian, L. D., Yao, T. D. & Zhang, X. P. 1996 $\Delta^{18}O$ in precipitation and moisture sources upon the Tibetan Plateau. *Cryosphere* **21**, 33–39.

Wels, C., Cornett, R. J. & Lazerte, B. D. 1991 Hydrograph separation, a comparison of geochemical and isotopic tracers. *J. Hydrol.* **122**, 253–274.

Wenninger, J., Uhlenbrook, S., Tilch, N. & Leibundgut, C. 2004 Experimental evidence of fast groundwater responses in a hillslope/floodplain area in the Black Forest Mountains, Germany. *Hydrol. Process.* **18**, 3305–3322.

Williams, M. W., Knauf, M., Caine, N., Liu, F. & Verplanck, P. L. 2006 Geochemistry and source waters of rock glacier outflow, Colorado Front Range. *Permafr. Periglac. Process.* **17**, 13–33.

Wu, S. S., Yao, Z. J., Huang, H. Q., Liu, Z. F. & Chen, Y. S. 2013 Glacier retreat and its effect on stream flow in the source region of the Yangtze River. *J. Geogr. Sci.* **23**, 849–859.

Yao, T. D., Wang, Y. Q., Liu, S. Y., Pu, J. C., Shen, Y. P. & Lu, A. X. 2004 Recent glacial retreat in High Asia in China and its impact on water resource in Northwest China. *Sci. China Ser. D* **47**, 1065–1075.

Yao, Z. J., Liu, Z. F., Huang, H. Q., Liu, G. H. & Wu, S. S. 2014 Statistical estimation of the impacts of glaciers and climate change on river runoff in the headwater of Yangtze River. *Quat. Int.* **336**, 89–97.

Ye, Q. H., Kang, S. C., Chen, F. & Wang, J. H. 2006 Monitoring glacier variations on Geladandong mountain, central Tibetan Plateau, from 1969 to 2002 using remote-sensing and GIS technologies. *J. Glaciol.* **52**, 537–545.

Yurtsever, Y. 2000 Environmental isotopes in the hydrological cycle. Vol 6, Modelling. pp. 495–496. http//www-naweb.iaea.org/napc/ih/documents/global_cycle/Environmental%20Isotopes%20in%20the%20Hydrological%20Cycle%20Vol%206.pdf.

Zhang, Y., Liu, S. Y., Xu, J. L. & Shangguan, D. H. 2008 Glacier change and glacier runoff variation in the Tuotuo River basin, the source region of Yangtze River in western China. *Environ. Geol.* **56**, 59–68.

Zhao, P., Tang, X. Y., Zhao, P., Wang, C. & Tang, J. L. 2013 Tracing water flow from sloping farmland to streams using oxygen-18 isotope to study a small agricultural catchment in southwest China. *Soil Tillage Res.* **134**, 180–194.

First received 9 April 2015; accepted in revised form 27 August 2015. Available online 22 October 2015